C.E. SACLAY
DSM

SERVICE DE PHYSIQUE NUCLEAIRE

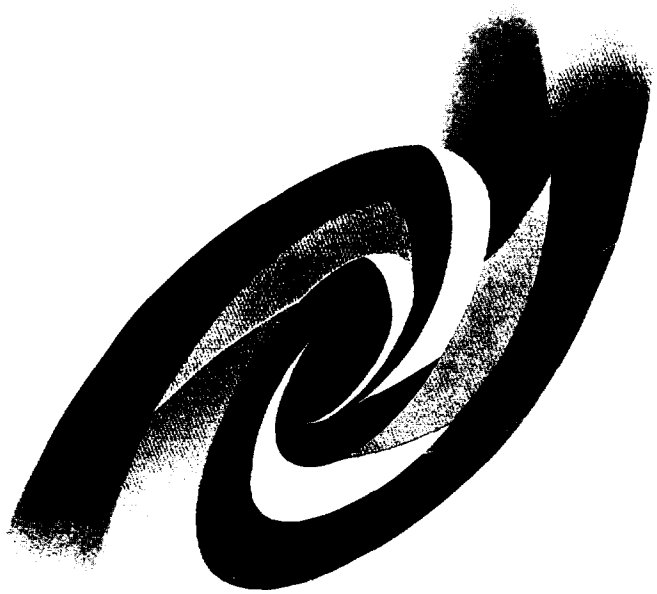

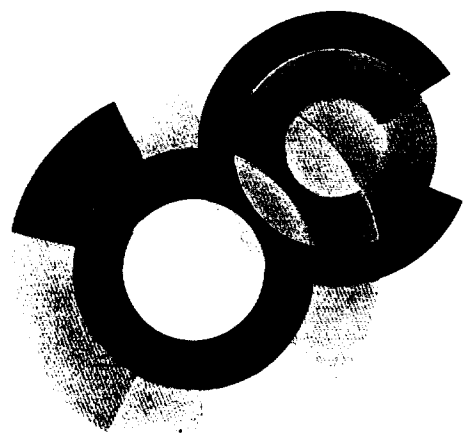

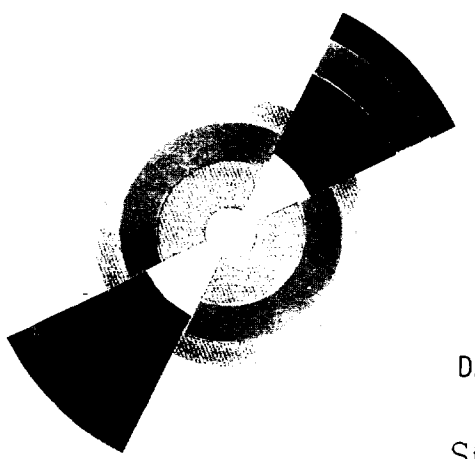

DAPNIA/SPhN-96-19 06/1996

Study of three nucleon mechanisms in the photodisintegration of ^{3}He

G.Audit , A. Braghieri , N. D'Hose , V. Isbert , S. Kerhoas , J.M. Laget , M. Mac Cormick , L.Y. Murphy , A. Panzeri , P. Pedroni , T.Pinelli , G. Tamas , J. Ahrens , J.R.M. Annand , R. Crawford , P. Grabmayr , S.J. Hall , J.D. Kellie ,

DAPNIA

VOL 28 № 2 2

Le DAPNIA (**D**épartement d'**A**strophysique, de physique des **P**articules, de physique **N**ucléaire et de l'**I**nstrumentation **A**ssociée) regroupe les activités du Service d'Astrophysique (SAp), du Département de Physique des Particules Elémentaires (DPhPE) et du Département de Physique Nucléaire (DPhN).

Adresse : DAPNIA, Bâtiment 141
CEA Saclay
F - 91191 Gif-sur-Yvette Cedex

Submitted to Nuclear Physics B

Study of three nucleon mechanisms in the photodisintegration of ^{3}He

G.Audit [a], A. Braghieri [b], N. D'Hose [a], V. Isbert [a], S. Kerhoas [a], J.M. Laget [a], M. Mac Cormick [a,1], L.Y. Murphy [a,2], A. Panzeri [b,c], P. Pedroni [b], T.Pinelli [b,c], G. Tamas [a], J. Ahrens [d], J.R.M. Annand [e], R. Crawford [e], P. Grabmayr [f], S.J. Hall [e], J.D. Kellie [e],

[a] *CEA-DAPNIA/SPhN, C.E. Saclay, 91191 Gif sur Yvette, France.*

[b] *INFN, Sezione di Pavia, Via Bassi 6, 27100 Pavia, Italy.*

[c] *Dipartimento Fisica Nucleare e Teorica, Università di Pavia, via Bassi 6, 27100 Pavia, Italy.*

[d] *Institut für Kernphysik, Universität Mainz, 55099 Mainz, Germany.*

[e] *Department of Physics and Astronomy, University of Glasgow, UK*

[f] *Physikalisches Institut, Universität Tübingen, 72076 Tübingen, Germany.*

Abstract

The cross section of the ^{3}He$(\gamma,pp)n$ reaction has been measured for the first time over a wide photon energy and proton angular range (200 MeV$\leq E_\gamma \leq$800 MeV; $20° \leq \vartheta_p^{lab} \leq 160°$) using the large acceptance detector DAPHNE at the tagged photon facility of the MAMI microtron in Mainz. The wide kinematical coverage of the measurement has allowed a detailed analysis of three nucleon absorption mechanisms. A model developed by Laget explains the main characteristics of the data in the Δ resonance region.

PACS number(s): 25.20.Dc; 25.10+s 21.45.+v

Keywords: NUCLEAR REACTIONS ^{3}He(γ,pp)n; E_γ =200 - 800 MeV; measured σ for three nucleon absorption mechanisms

Correspondence to: Dr. P. Pedroni, INFN-Sezione di Pavia, via Bassi 6, 27100 Pavia, Italy; E-mail: PEDRONI@PAVIA.INFN.IT, telephone: +39 382 507428, fax: +39 382 423241

[1] present address: GANIL, Bd. Henri Bequerel, 14000, Caen, France.

[2] present address: The George Washington University, Washington DC 20052 USA

1 Introduction

The nature of three-body (3N) forces in nuclei is still an open problem. The main evidence for the need of such a mechanism lies in the failure of two-body (2N) forces to explain the binding energy of light nuclei. As early as 1957 Fujita and Miyazawa [1] proposed diagram Ib of Fig.1 as a mechanism for 3N forces not reducible to sequential 2N interactions. This diagram can be understood as a correction to the 2π exchange part of the N-N potential (diagram Ia of Fig.1) due to the presence of a third nucleon. When included in the calculations of the binding energy of the three nucleon systems, this mechanism brings the theoretical values into better agreement with the experimental values, but still slightly overestimates them [2].

One of the most valuable reactions for studying 3N dynamics is the three-body photodisintegration of ^{3}He in kinematics where the photon momentum is shared by the 3 nucleons. To ensure gauge invariance, the photon has to be coupled to each of the objects which are exchanged and has to be attached to any of the branches of diagram Ib. These photoreaction mechanisms can be put into two main categories:

- photoproduction on one nucleon of a pion which is absorbed sequentially by the two others(diagram Ic of Fig.1 referred to as '3N(2-step)')
- direct photoproduction of two virtual pions on one nucleon with subsequent reabsorption by the other nucleons (diagram Id referred to as '3N(2π)')

All other contributions, which impose a pre-existing Δ, can be neglected since the probability of isobaric mixing in the ground state of the very light nuclei is estimated by all models to be very small (a few % at maximum; see for instance, ref. [3]).

The classification in '3N(2-step)' and '3N(2π)' processes, that is done just for the simplicity in the writing and does not refer to any distinction between 'genuine' or 'non-genuine' 3N mechanisms, is valuable because their contributions can be partially disentangled. In the '3N(2π)' process the 2 pions are always off-shell, while in the '3N(2-step)' process the photoproduced pion can propagate on-shell giving rise to a singularity in the cross section for certain kinematical configurations.

The first ^{3}He$(\gamma, pp)n$ experiments [4] used photons with an energy of around 350 MeV and the protons were detected in coincidence in two magnetic spectrometers. The '3N(2-step)' mechanism corresponding to the photoproduction of a pion on one nucleon, and its subsequent reabsorption on the remaining two-nucleon pair, was selected by choosing the precise kinematical region where the exchanged pion propagates on-shell. The results were consistent with the predictions of multiple-scattering calculations [5], but the clear signature

of this effect was weakened by final-state interactions between outgoing nucleons which were restricted to move within the reaction plane. Another similar experiment [6], in the photon energy range 90 - 200 MeV, has confirmed that the '3N(2-step)' mechanism is needed in order to adequately describe the data.

Inclusive measurements of the ^{3}He(γ, p) cross section [7,8] suggest that, apart from the dominant 2N absorption on a correlated (n, p) pair, a sizeable contribution to the total photodisintegration cross section comes from 3N photoabsorption mechanisms.

More recent experiments have also attempted to explore the 3N mechanisms over wider kinematical regions. Ref. [9] reports a measurement in the photon energy range 200 - 500 MeV using the proton spectrometer TAGX, which has a solid angular acceptance of $\simeq \pi$ sr. The yields for 2N and 3N processes were extracted by fitting the undetected neutron momentum distribution and a three-body phase space was assumed for the latter mechanism. Linearly polarized photons have also been used at LEGS in the energy range 235-305 MeV with a proton detector of acceptance $\simeq \pi/3$ sr [10]. In this case 3N mechanisms were also necessary to describe both the angular distributions and the beam asymmetry of *pp* events. Experiments on pion absorption in ^{3}He were also carried out to investigate the same basic 3N mechanisms [11]–[13] which were found to give a significant contribution to the total pion absorption cross section.

The aim of the present experiment was to study the γ^3He$\rightarrow$ *ppn* reaction over a large photon energy range (200-800 MeV) with a large momentum and angular acceptance for the outgoing particles. A total of 10^6 events were recorded enabling the photon energy dependence to be studied in detail. The results of the complementary experiment γ^3He$\rightarrow$ *pd* have already been published [14].

2 Experimental set-up

The present experiment was performed with the large acceptance (3.7π sr) detector DAPHNE [15], built by DAPNIA-SPhN at Saclay and the INFN-Sezione di Pavia and was used in conjunction with the tagged photon facility [16], installed by Glasgow University at the race-track microtron MAMI [17] at Mainz.

The tagged photon beam was produced by bremsstrahlung of the 855 MeV electrons from MAMI on a thin gold convertor of 10^{-4} radiation lengths. The tagging system covers a photon energy range of 50-800 MeV in 352 channels each having an energy resolution of $\simeq 2$ MeV. The collimation of the photon beam gives an experimental tagging efficiency of about 55%. A total tagged

photon flux of $\simeq 10^7$/s over the full energy range was used. The photon flux was continuously measured with the aid of detectors placed in the beam downstream of the hadronic detector. Incident photons were converted into e^+e^- pairs by a 0.5 mm copper convertor and detected in coincidence by two plastic scintillator layers placed directly behind. The photon detection efficiency of this device was regularly measured, at low beam intensity, by comparison with a 100% efficient lead-glass detector. The absolute number of tagged photons was determined with a precision of $\pm 2\%$ [18].

The DAPHNE device has a central tracking detector, consisting of three coaxial cylindrical multiwire proportional chambers, surrounded by a segmented cylindrical scintillator ΔE-E telescope for charged particle identification [19]. Finally there is a scintillator-absorber sandwich that is designed to enhance the π^0 detection efficiency and the particle identification. The main characteristics of the detector are :
- a large angular acceptance (polar acceptance : $22° \leq \theta \leq 158°$ and azimuthal acceptance $0° \leq \phi \leq 360°$);
- an excellent angular resolution for charged particles ($\Delta\theta$ (FWHM) $\leq 1°$, $\Delta\phi$ (FWHM) $\simeq 2°$);
- a large momentum acceptance (for protons : $P_p \geq 300$ MeV/c; for pions : $P_\pi \geq 78$ MeV/c) ;
- a good proton/pion particle discrimination for proton momenta $P_p \leq 900$ MeV/c;
- a good proton momentum resolution ($\Delta P_p/P_p$=2.5-10% in the measured range);
- modest π^0 efficiency ($\simeq$20% when both photons from the π^0 decay are detected in coincidence).

The liquid ^{3}He target, maintained at 2.65 K and 556 mbar, is contained in a Mylar cylinder of dimensions 4.3 cm in diameter by 27.5 cm in length. The system consisted of a Gifford-Mac-Mahon ^{4}He refrigerator coupled to a Joule-Thomson expansion valve which provides the pressure reduction necessary in order to reach liquefaction. The cryogenic system was automatically regulated and all critical parameters relating to the target environment were continuously recorded [20]. Under operating conditions, the fluctuations in temperature were less than $5{\cdot}10^{-3}$ K, which ensured a stability in the target density of $\pm 0.5\%$.

3 Data Analysis

Since the photon energy and the momenta and directions of the two detected protons are known precisely, the *ppn* kinematics is overdetermined and a kinematic fit can be performed in order to eliminate all competing reactions in which pions are produced. Fig.2 shows the missing mass distribution of the

system γ^3He$\rightarrow$ ppX before and after this selection: a very clean separation was obtained between the channels with and without pions in the final state.

In order to avoid any contamination from the γ^3He$\rightarrow$ pd channel, the azimuthal angles of the 2 detected protons were required to differ from coplanarity by more than 5°. Moreover, in order to select precisely 3N photoabsorption mechanisms in the γ^3He$\rightarrow$ ppn channel, large momenta for the 3 outgoing particles, i.e higher than 300 MeV/c for the protons and 150 MeV/c for the neutron, were selected. The criteria for selected ppn events define the DAPHNE acceptance and are summarized in Table 1.

TABLE 1
DAPHNE acceptance for p_1p_2n events

$22° \leq \theta_{p1,2} \leq 158°$
$0° \leq \phi_{p_{1,2}} \leq 360°$ and $\lvert\phi_{p_1} - \phi_{p_2}\rvert \geq 5°$
$P_{p1,2} \geq [0.023 \times (\theta_{p_{1,2}} - 90°)^2 + 300]$ MeV/c
$P_{p1,2} \leq [0.025 \times (\theta_{p_{1,2}} - 90°)^2 + 840]$ MeV/c
$P_n \geq 150$ MeV/c

The number of the selected ppn events is corrected for geometrical effects due to the extended target, for the efficiency of wire chambers ($\simeq$ 97%) and of the particle identification method (90 - 50% depending on the proton angle and momentum). All systematic errors taken into account in the cross section evaluation, equal to those of previous similar experiments [14,18], are listed in Table 2.

TABLE 2
Systematic errors

Number of photons	±2%
Target thickness	±0.5%
Wire chamber efficiency	±1%
Proton identification method (depending on photon energy)	±1 − 5%

4 Results

4.1 Total cross section

The total cross section for the γ^3He$\rightarrow$ *ppn* reaction integrated over the DAPHNE acceptance, shown in Fig.3, has a pronounced peak at $E_\gamma \simeq 320$ MeV which clearly indicates that this reaction is governed, in this region, by the intermediate Δ excitation. No other structure is observed in the higher second resonance region up to 800 MeV.

It is important to note that the maximum at 320 MeV is not an artefact of the cuts in the phase space. The solid line in Fig.4 shows the DAPHNE acceptance if a uniform 3N phase space distribution is assumed. Its E_γ dependence is considerably different from that of the cross section, starting from 16% at 200 MeV, going up to a maximum of 56% at 500 MeV and then decreasing slowly to 35% at 800 MeV due to the 900 MeV/c limitation imposed on the proton momenta for good identification [19].

Since the analysis cannot separate 2N absorption in which the third nucleon has a high momentum (due either to Fermi motion or final state interactions (FSI) from 3N mechanisms, a model was used to subtract it from the data. To obtain the total cross section for 3N photoabsorption it was assumed that:

- the 2N absorption cross section is given by the Laget model [5];
- there is no interference between 2N and 3N mechanisms;
- 3N mechanisms follow an uniform 3N phase space distribution.

The results are shown in Fig.5 together with the total contribution of 3N absorption recently evaluated by the TAGX experiment [9].

The discrepancy between our data and TAGX could be attributed to the fact that the model used in ref. [9] for the 2N/3N separation systematically underestimates the experimental undetected neutron momentum distributions, as can be seen in Fig.2 of [9]. Moreover, in the same work it is assumed that events with a low neutron momentum are mostly due to 2N mechanisms but Sandorfi and Leideman [22] have recently pointed out that the LEGS results do not support this simple hypothesis.

According to our results, in the total phase space the 3N absorption strength in ^{3}He represents about 36% of the 2N strength, where the 2N absorption is taken as $\sigma[(\gamma^3He \rightarrow pn)p_{spect.}] = 1.68 \times \sigma[\gamma d, pn]$ (see ref [7]). This fraction is is quite large and confirms the order of magnitude measured in pion absorption experiments [11]–[13].

The full curve in Fig.3 shows the integration of Laget's model [5] by a Monte Carlo method over the DAPHNE acceptance. This model is based on a diagrammatic expansion which takes into account the following processes:

- 2N mechanisms whose contribution is indicated by a dotted line in Fig.3;
- 3N mechanisms of 2 types ('3N(2-step)' and '3N(2π)', as previously discussed).

The full model was not used in the final calculation as excessively long computing times were necessary (about 5 min of CPU per point on a Cray computer). For computing time reasons, the integration over the Fermi motion at the pion production vertex was not included in the Monte Carlo calculation while it is included in the pion absorption loop. In view of this approximation, the agreement between the experiment and the model is quite good and at least this model reflects the general trends. We see, in particular, that the main contribution to the 3N cross section in this model is given by the '3N(2 step)' process. This dominance was already noted by Carrasco and Oset in their calculations of photon absorption in nuclei [21].

4.2 3N mechanism study

The above analysis allows the strength of the 3N mechanisms to be extracted but does not produce a simple experimental signature of these mechanisms. The possibility of finding such a signature is pursued below.

In diagram Id of Fig.1 the two exchanged pions are always off-shell while in diagram Ic there exists a small phase space region where the first photoproduced pion propagates on-mass shell before being reabsorbed by the remaining pair, thus giving rise to a singularity in the cross section. The aim of a previous experiment was to find this singularity [4], but in that case the results were considerably affected by FSI's of the detected coplanar protons.

The $^3He(\gamma, ppn)$ data from the present experiment can be displayed conveniently in a triangular Dalitz plot as shown in Fig.6 for $E_\gamma = 400 \pm 25$ MeV. This plot shows two densely populated areas due to nucleon rescattering in the final state. By selecting the central region delimited by the two parallel lines in Fig.6 one can remove most of these FSI effects.

For these selected events, under the assumption that the main contribution to the '3N(2-step)' process is given by the photoproduction of a π^+ over a stationary proton ($\gamma + p \rightarrow n + \pi^+$) followed by the reabsorption of this π^+ by a 'np' pair at rest ($\pi^+ + d \rightarrow p + p$) we can reconstruct the invariant mass m_X of this exchanged pion, which is given by:

$$m_X^2 = (E_\gamma + m_p - E_n)^2 - (\vec{p_\gamma} - \vec{p_n})^2$$

If a peak appears at a mass $m_X^2 = m_\pi^2$, this is a clear signature of the exchange of a real pion which corresponds to the '3N(2-step)' mechanism. This is clearly the case in Fig.7 where, for $E_\gamma = 300$ MeV, a well pronounced peak stands out from the uniform phase space distribution.

The theoretical shape predicted by the Laget model does not reproduce the experimental one since, as was previously mentioned, the peak is broadened by the Fermi motion of the absorbing 'np' pair, and this effect has not yet been taken into account. However this model, which reproduces the main features of the total cross section, confirms the predominant role of this '3N(2-step)' process.

Above $E_\gamma = 500$ MeV the corresponding experimental peak does not show up so clearly and so definitive conclusions cannot be drawn. The theoretical model predicts the '3N(2-step)' process dominance but, as it can be seen in Fig.3, the shape of the total cross section is not well reproduced and other important diagrams, with the intermediate excitation of higher baryon resonances, should be included.

5 Conclusion

The use of a 100% duty factor tagged photon beam coupled with a large acceptance detector has allowed, for the first time, a high precision measurement of the ^{3}He(γ, ppn) reaction over a wide energy and angular range.

From both our data and the Laget model, it can be seen that, in the Δ region, the 3N photodisintegration of ^{3}He is dominated by a '3N(2-step)' mechanism which corresponds to the photoproduction on one nucleon and the reabsorption of the produced pion by the two other nucleons while, above 500 MeV, this mechanism was not identified experimentally.

This data set provides a strong constraint on further theoretical studies on the role of multinucleon processes.

Acknowledgements

We are grateful to all the MAMI machine crew for the excellent beam quality that was maintained throughout the experiment. Participants from Glasgow

acknowledge the financial support given by the Science and Engineering Research Council.

References

[1] I. Fujita and H. Miyazawa, Prog. Theor. Phys. 17 (1957) 360.

[2] A. Stadtler et al., Phys. Rev. C51 (1995) 2896.

[3] M.T. Peña et al., Phys. Rev. C48 (1993) 2208.

[4] G. Audit et al., Phys. Lett. B227 (1989) 331; Phys. Lett. B312 (1993) 57; Phys. Rev. C44 (1991) R575.

[5] J.M. Laget, J. of Phys. G14 (1988) 1445; Nucl. Phys. A497 (1989) 391.

[6] A.J. Sarty et al., Phys. Rev. C47 (1993) 459.

[7] N. d'Hose et al., Phys. Rev. Lett. 63 (1989) 856.

[8] C. Ruth et al., Phys. Rev. Lett. 72 (1994) 617.

[9] T. Emura et al., Phys. Rev. Lett. 73 (1994) 404.

[10] D.J. Tedeschi et al., Phys. Rev. Lett. 73 (1994) 408.

[11] G. Backenstoss et al., Phys. Rev. Lett. 55 (1985) 2782; Phys. Lett. B222 (1989) 7; P. Weber et al., Nucl. Phys. A534 (1991) 541.

[12] K.A. Aniol et al., Phys. Rev. C33 (1986) 1714.

[13] L.C. Smith et al., Phys. Rev. C40 (1989) 1347; S. Mukhopadhyay et al., Phys. Rev. C43 (1991) 957.

[14] V. Isbert et al., Nucl. Phys. A578 (1994) 525.

[15] G. Audit et al., Nucl. Instr. and Meth. A301 (1991) 473.

[16] I. Anthony et al., Nucl. Instr. and Meth. A301 (1991) 230; S.J. Hall et al., Nucl. Instr. and Meth. A368 (1996) 698.

[17] H. Herminghaus et al., Nucl. Instr. and Meth. A138 (1976) 1.

[18] R. Crawford et al., Nucl. Phys. A, in press.

[19] A. Braghieri et al., Nucl. Instr. and Meth. A343 (1994) 623.

[20] B. Hervieu et al., Comptes Rendus des quatrièmes journées d'Aussois, Aussois 1993, ed. CNRS Grenoble.

[21] R.C. Carrasco and E. Oset, Nucl. Phys. A536 (1992) 445; Nucl. Phys. A541 (1992) 585.

[22] A. Sandorfi and W. Leidemann, Phys. Rev C53 (1996) 1506.

Figure captions

(i) Feynman diagrams representing the 2π exchange part of the two-body N-N potential (Ia), a three body force involving 2π exchange (Ib) and the three-body photoabsorption mechanisms taken into account in a calculation by Laget [5] (Ic and Id).

(ii) Missing mass distribution for $^3He(\gamma, pp)X$ events before and after the kinematic fit performed in order to select the γ ^{3}He$\rightarrow$ *ppn* channel.

(iii) The total cross section of the γ ^{3}He$\rightarrow$ *ppn* channel integrated over the DAPHNE acceptance (black squares) is compared to the theoretical predictions of Laget.

(iv) DAPHNE acceptance probability for the γ ^{3}He$\rightarrow$ *ppn* channel if a uniform phase space distribution is assumed for the outgoing nucleons.

(v) The total cross section for 3N photoabsorption estimated from the experimental data is compared to the results obtained by the TAGX experiment [9].

(vi) Triangular Dalitz plot at 400 MeV : the three axes are the c.m. kinetic energies of proton$_1$, proton$_2$, and neutron normalized to the total c.m. energy. Events in the region between the 2 parallel lines were selected for the study of 3N mechanisms.

(vii) Distribution, at 300 MeV, of the invariant mass of the object X which is exchanged between the proton and the neutron-proton pair as discussed in the text.

fig.1

I a

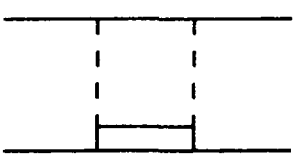

I b

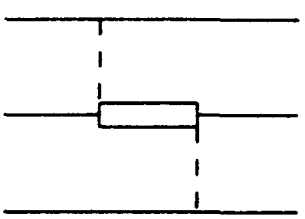

I c

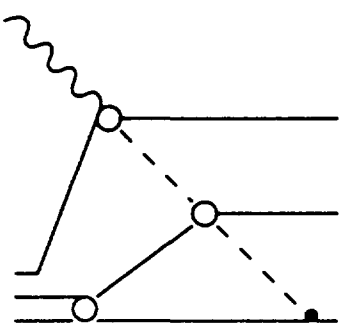

I d

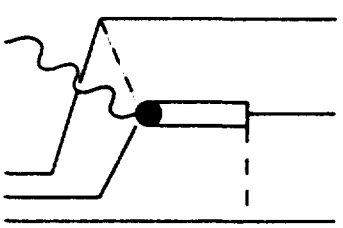

fig.2

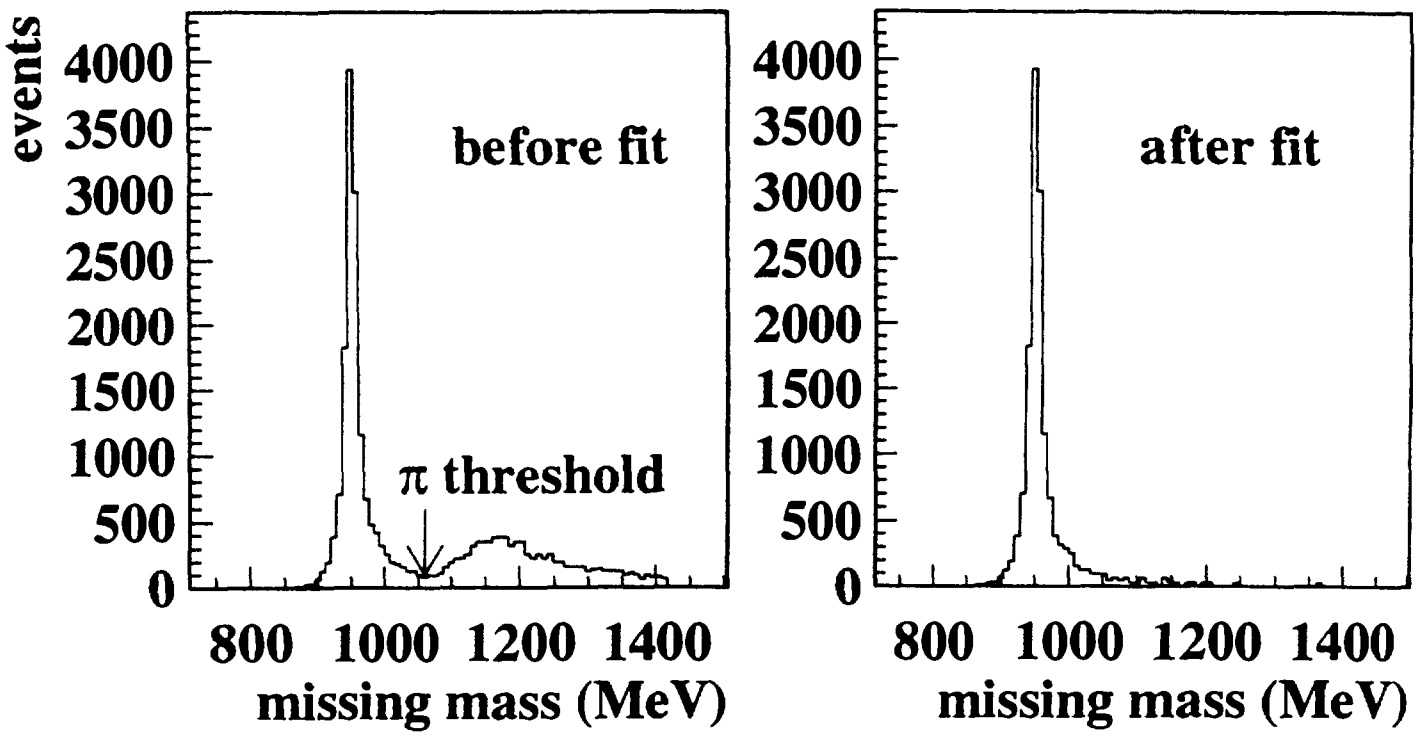
events
4000
3500
3000
2500
2000
1500
1000
500
0
before fit
π threshold
800 1000 1200 1400
missing mass (MeV)
4000
3500
3000
2500
2000
1500
1000
500
0
after fit
800 1000 1200 1400
missing mass (MeV)

fig.3

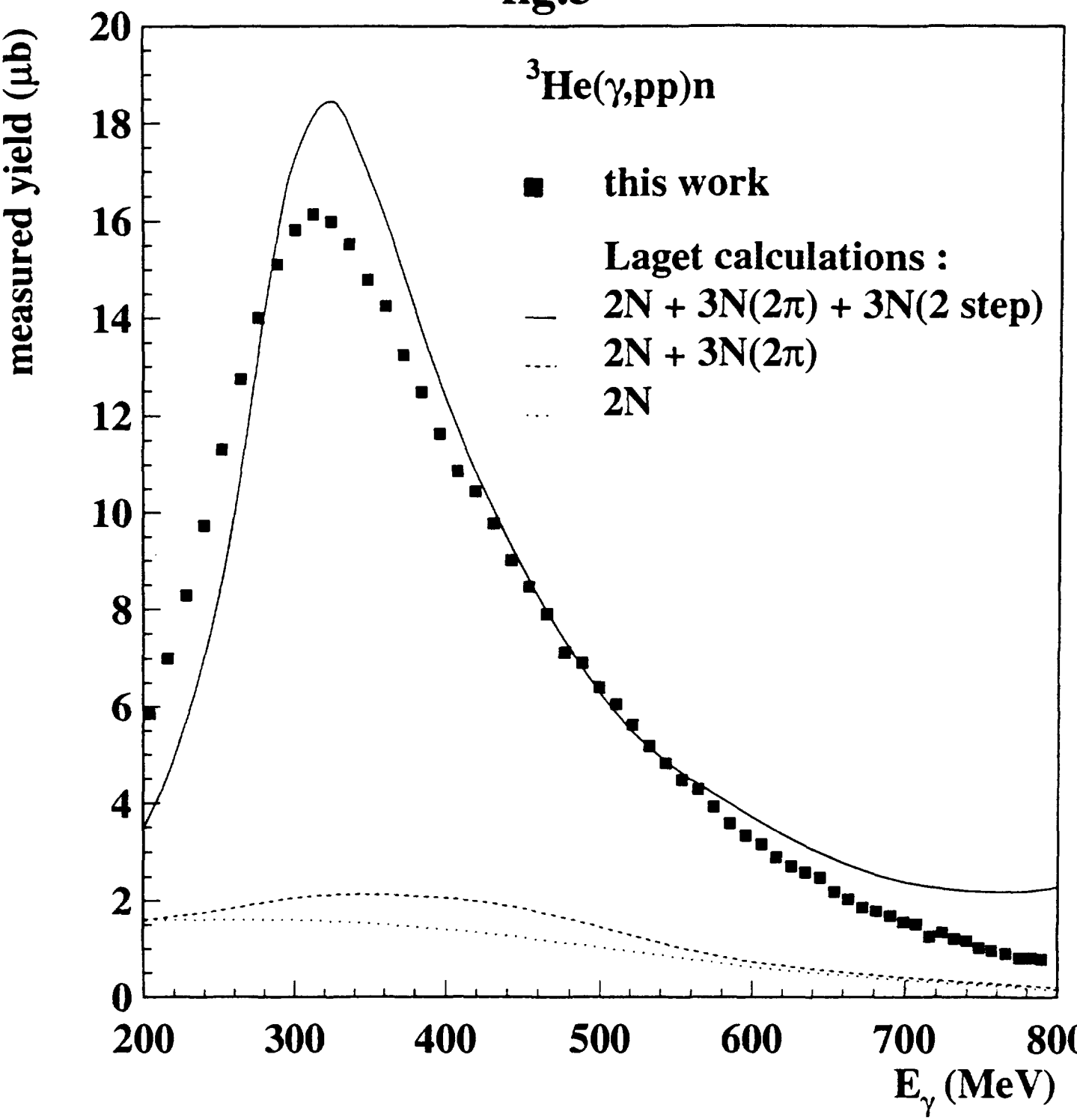
measured yield (μb)
20
18
16
14
12
10
8
6
4
2
0
200
300
400
500
600
700
800
E_γ (MeV)
^{3}He(γ,pp)n
this work
Laget calculations :
2N + 3N(2π) + 3N(2 step)
2N + 3N(2π)
2N

fig.4

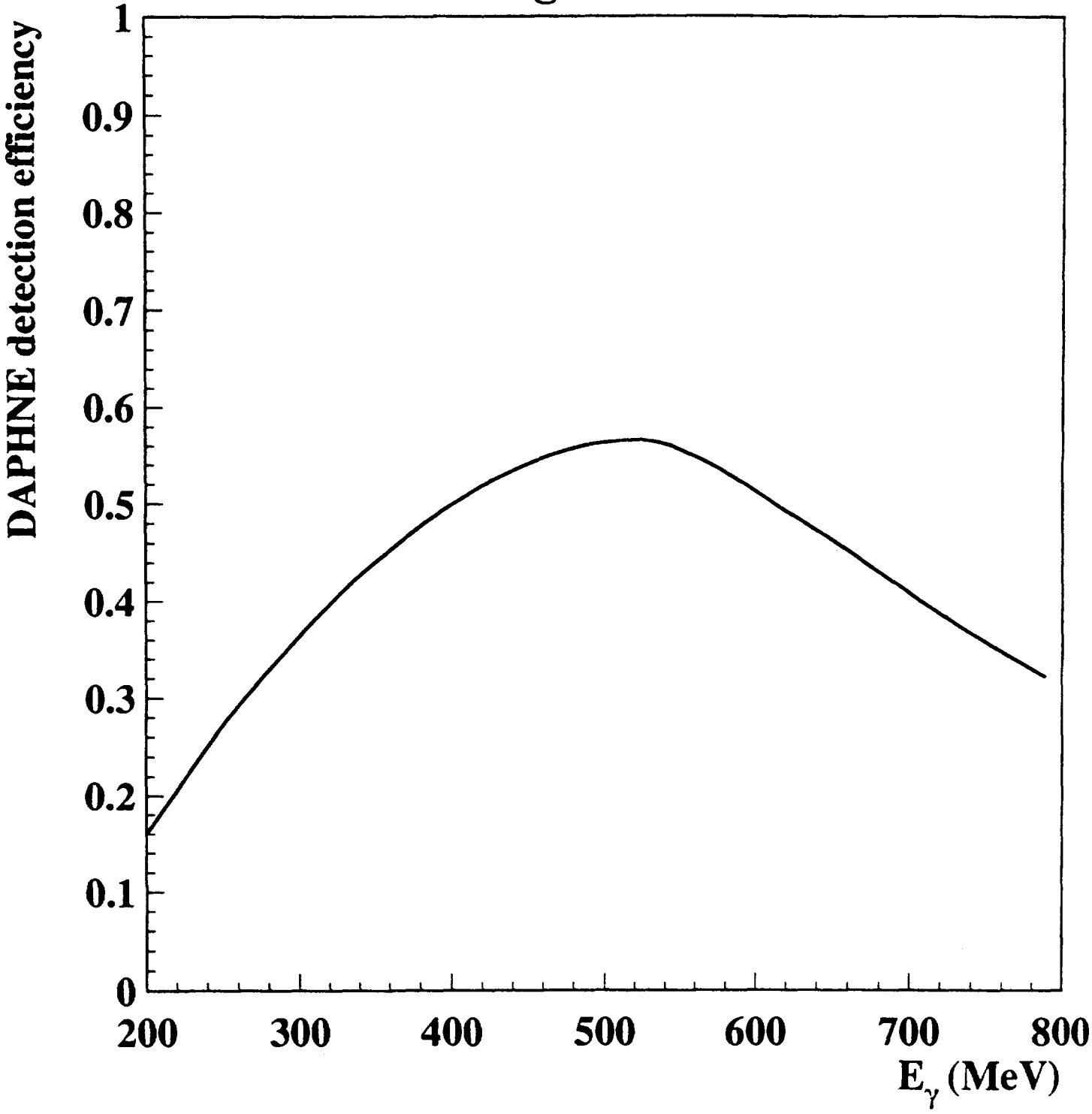
DAPHNE detection efficiency
1
0.9
0.8
0.7
0.6
0.5
0.4
0.3
0.2
0.1
0
200
300
400
500
600
700
800
E_γ (MeV)

fig.5

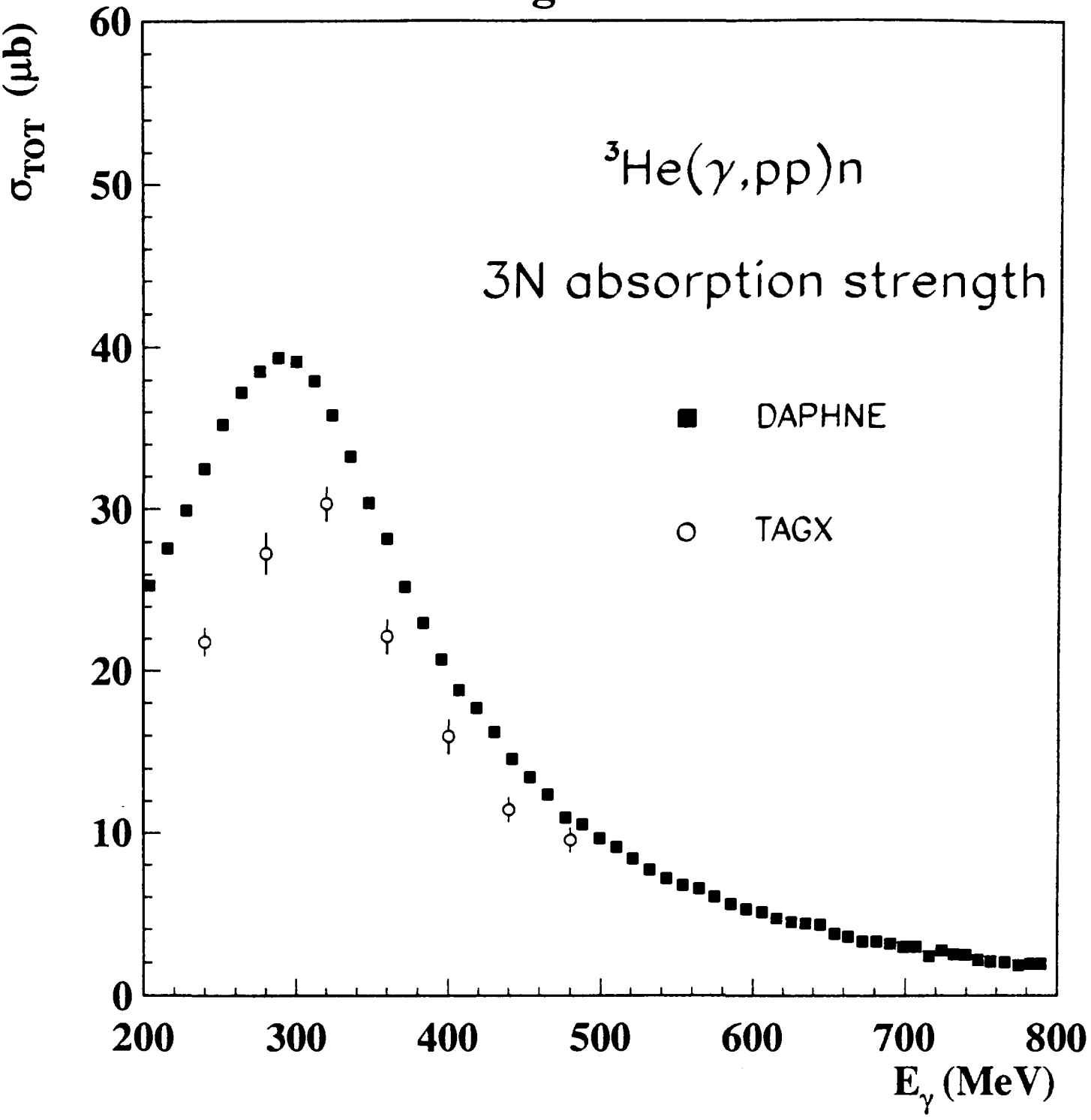
σ_{TOT} (μb)
60
50
40
30
20
10
0
200
300
400
500
600
700
800
E_γ (MeV)
^{3}He(γ,pp)n
3N absorption strength
DAPHNE
TAGX

fig.6

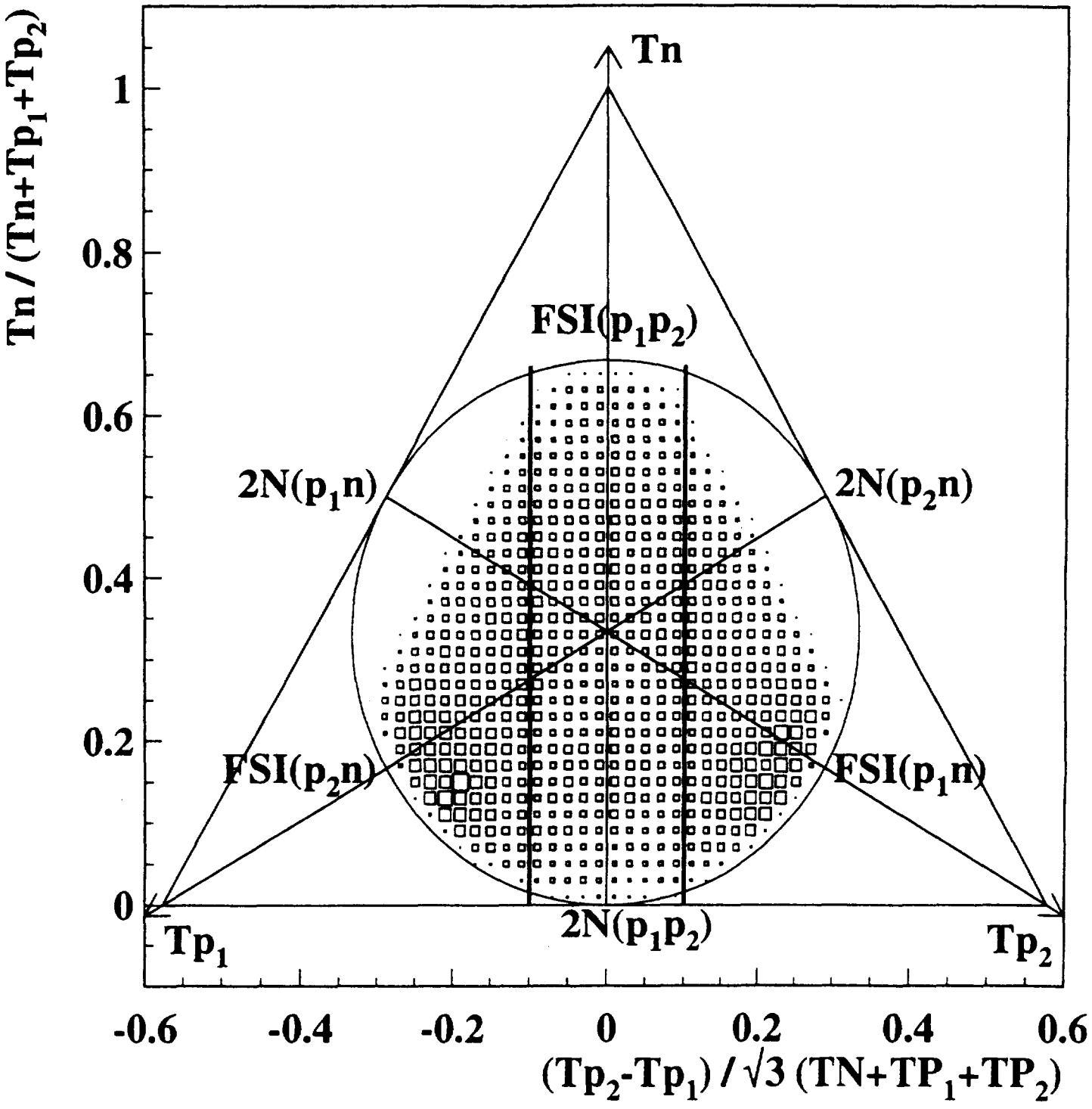
Tn / (Tn+Tp1+Tp2)
1
0.8
0.6
0.4
0.2
0
Tn
FSI(p1p2)
2N(p1n)
2N(p2n)
FSI(p2n)
FSI(p1n)
Tp1
2N(p1p2)
Tp2
-0.6
-0.4
-0.2
0
0.2
0.4
0.6
(Tp2-Tp1) / √3 (TN+TP1+TP2)

fig.7

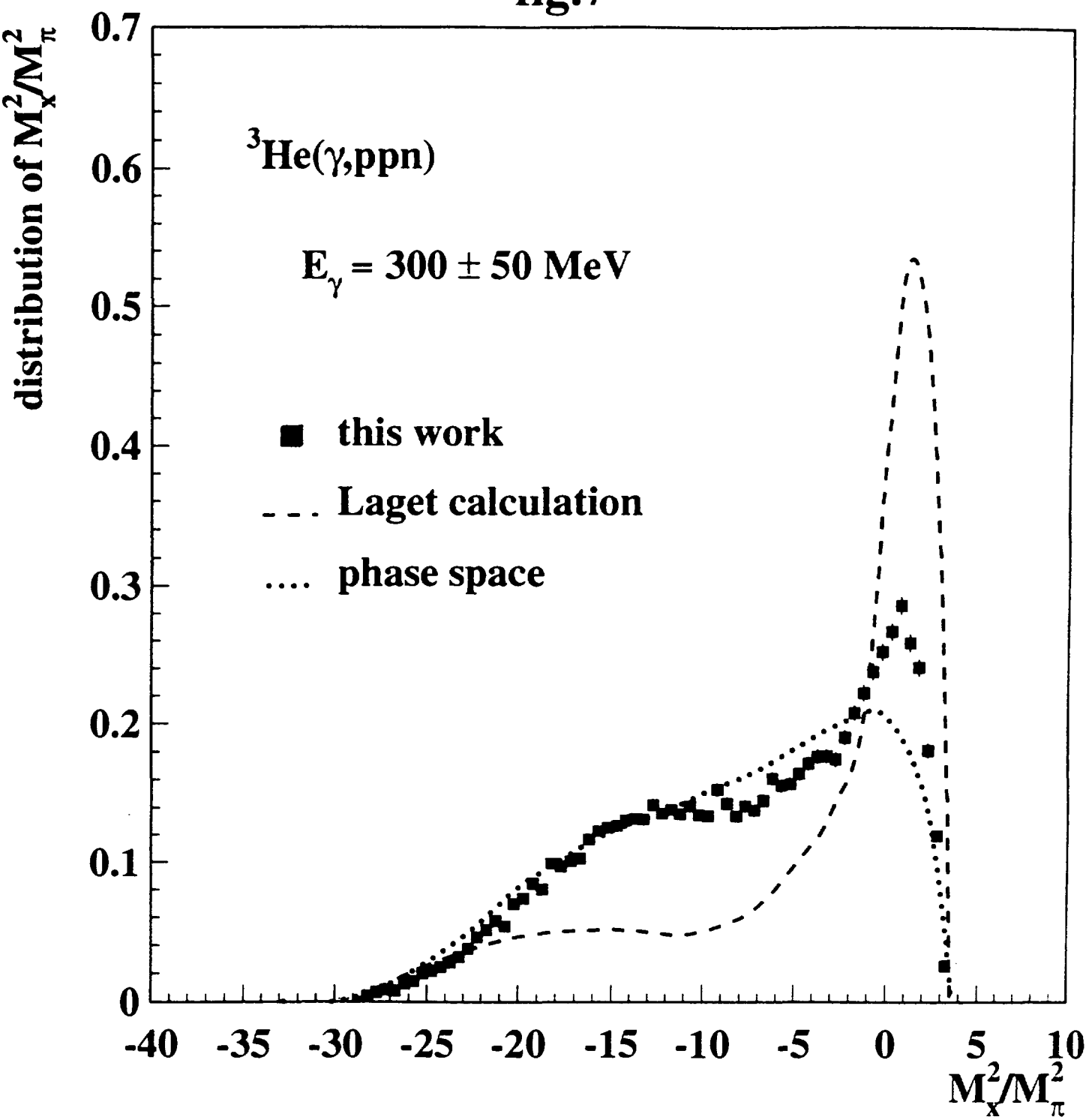
distribution of M_x^2/M_π^2
0.7
0.6
0.5
0.4
0.3
0.2
0.1
0
^{3}He(γ,ppn)
$E_\gamma = 300 \pm 50$ MeV
this work
Laget calculation
phase space
-40
-35
-30
-25
-20
-15
-10
-5
0
5
10
M_x^2/M_π^2